Asian Journal of Chemistry; Vol. 25, No. 16 (2013), 9199-9202

ASIAN JOURNAL OF CHEMISTRY

http://dx.doi.org/10.14233/ajchem.2013.15147B

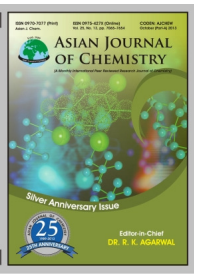

An Improved Calcination Route to Synthesize Carbon Doped Mesoporous TiO_2 and Its Photocatalytic Activity Under Visible Light

S.Z. HU[1,*], F.Y. LI[1], Z.P. FAN[1] and J. ZHANG[2]

[1]Institute of Eco-environmental Sciences, Liaoning Shihua University, Fushun 113001, P.R. China
[2]School of Petrochemical Engineering, Liaoning Shihua University, Fushun 113001, P.R. China

*Corresponding author: Tel: +86 24 23847473; E-mail: hushaozheng001@163.com

(*Received*: 15 January 2013; *Accepted*: 20 September 2013) AJC-14144

Carbon doped mesoporous TiO_2 was prepared by an improved calcination route. X-Ray diffraction, UV-visible spectroscopy, TEM, X-ray photoelectron spectroscopy and nitrogen adsorption were used to characterize the prepared TiO_2 samples. Citric acid was used as not only carbon source but also the pore-forming agent. The photocatalytic activities were tested in the degradation of an aqueous solution of a reactive dyestuff, methylene blue, under both UV and visible light. The carbon doped mesoporous TiO_2 prepared by improved calcination route showed much higher photocatalytic activity than that of catalyst prepared by conventional calcination route and neat TiO_2 under visible light. A possible mechanism for the photocatalysis was proposed.

Key Words: Carbon doping, TiO_2, Photocatalysis, Visible light, Improved calcination route.

INTRODUCTION

TiO_2 is widely used for the mineralization of environmental pollutants including organic or inorganic and it exhibits strong oxidation activity under ultraviolet light. However, with a wide band gap energy of 3.0-3.2 eV, TiO_2 can not be activated to generate photoexcited electrons and holes to promote redox reaction unless it is irradiated by ultraviolet. In order to utilize wider range of solar energy, lots of efforts have been made to narrow band gap by doping non-metal elements. As a result, visible light sensitive photocatalytic materials could be achieved by narrowing band gap *via* overlapping between O_{2p} orbital and $C_{2p}/N_{2p}/S_{3p}$ orbital[1-3]. Besides, transition metal doping[4,5] has also been effective to develop high photocatalytic activity by decelerating recombination rate between photo-excited electrons and holes.

The incorporation of carbon atoms into TiO_2 can be easily achieved with excellent reproducibility and great applicability[6], carbon-doped TiO_2 has received steadily growing attention. Irie and coworkers prepared carbon-doped anatase TiO_2 powders by oxidative annealing of TiC under O_2 flow at 600 ºC. The prepared catalysts showed photocatalytic activities for the decomposition of 2-propanol to CO_2 *via* acetone under visible light irradiation (400-530 nm)[7]. Sakthivel and Kisch synthesized carbon-doped TiO_2 by the hydrolysis of titanium tetrachloride with tetrabutylammonium hydroxide followed by calcination at 400 and 500 ºC. In the degradation of 4-chlorophenol by artificial light ($\lambda \geq 455$ nm) the catalyst powders have a high photocatalytic activities[6].

However, on the other hand, the synthesis methods for carbon doping are usually quite complicated and needing elaborate controlling. It is a challenge to prepare carbon-doped TiO_2 by a convenient method. In this work, carbon doped mesoporous TiO_2 was prepared by an convenient method, temperature-programmed calcination method, using citric acid as raw material. The photocatalytic performances of prepared samples were evaluated in the degradation of methylene blue under both UV and visible light.

EXPERIMENTAL

Carbon doped mesoporous TiO_2 nanoparticles were synthesized by sol-gel method. The analytical grade titanium isopropoxide [$Ti(OPri)_4$, AR], C_2H_5OH (AR), $C_6H_8O_7$ (citric acid, AR) and ammonia (25 %, AR) were used as raw materials. The process could be described as follows. Appropriate amount of $Ti(OPri)_4$ was added to the solution which contains citric acid and C_2H_5OH under constant stirring. Ammonia was used to adjust the pH value to 6-7. The total molar ratio of citric acid: C_2H_5OH: Ti was 2:2:1. After adjusting the pH value, the obtained solution was evaporated at 343 K to gradually form a clear gel precursor. This precursor was baked in the oven at 373 K for 12 h. The obtained solid sample was heated in muffle furnace to 180 ºC at a rate of 3 ºC min^{-1} and maintained at 180 ºC for 2 h. Then the sample was heated to 400, 500 and 600 ºC

at a rate of 5 ºC min^{-1}, respectively and maintained at corresponding temperature for 2 h. The obtained product was denoted as C-400, C-500 and C-600. For comparison, T-500 was prepared following the same procedure as in the synthesis of C-500 but in the absence of citric acid and ammonia. The direct calcination sample, C_d-500, was prepared by the same procedure as in the synthesis of C-500 but heated to 500 ºC at a rate of 5 ºC min^{-1} directly.

X-Ray diffraction patterns of the prepared TiO_2 samples were recorded on a Rigaku D/max-2400 instrument using Cu-K_α radiation (λ = 1.54 Å). UV-VIS spectroscopy measurement was carried out on a Jasco V-550 spectrophotometer, using $BaSO_4$ as the reference sample. TEM images were measured using a Philips Tecnai G220 model microscope. The Brunauer-Emmett-Teller (BET)-specific surface areas (S_{BET}) of the samples were determined through nitrogen adsorption at 77K (Micromeritics ASAP 2010). All the samples were degassed at 393K before the measurement. X-Ray photoelectron spectroscopy (XPS) measurements were conducted on a Thermo Escalab 250 XPS system with AlK_α radiation as the exciting source. The binding energies were calibrated by referencing the C 1s peak (284.6 eV) to reduce the sample charge effect. Photoelectrochemical experiments were carried out in a glass cell using a three-electrode system controlled by a VoltaLab 40 potentiostat (PGZ 301, Radiometer analytical).

Methylene blue (MB) was selected as model compound to evaluate the photocatalytic performance of the prepared TiO_2 particles in an aqueous solution under visible light irradiation. 0.1 g TiO_2 powders were dispersed in 100 mL aqueous solution of methylene blue (50 ppm) in an ultrasound generator for 10 min. The suspension was transferred into a self-designed glass reactor and stirred for 0.5 h in darkness to achieve the adsorption equilibrium. In the photoreaction under visible light irradiation, the suspension was exposed to a 110 W high-pressure sodium lamp with main emission in the range of 400-800 nm and air was bubbled at 130 mL/min through the solution. The UV light portion of sodium lamp was filtered by 0.5 M $NaNO_2$ solution. All runs were conducted at ambient pressure and 30 ºC. At given time intervals, 4 mL suspension was taken and immediately centrifuged to separate the liquid samples from the solid catalyst. The concentrations of methylene blue before and after reaction were measured by means of a UV-visible spectrophotometer at a wavelength of 665 nm. The percentage of degradation D % was determined as follows:

$$D\,\% = \frac{A_0 - A}{A_0} \times 100\,\% \quad (1)$$

where A_0 and A are the absorbances of the liquid sample before and after degradation, respectively.

RESULTS AND DISCUSSION

The XRD patterns of neat and C doped TiO_2 samples (Fig. 1) show that all TiO_2 samples were pure anatase phase, indicating that doping did not influence the crystal structure. The particle sizes of the catalysts were calculated by their XRD patterns according to the Debye-Scherrer equation[8]. The results indicated that the particle sizes of T-500, C_d-500, C-400, C-500 and C-600 were 11.6, 11.7, 10.3, 11.4 and 14.2 nm. The particle size increased gradually with increasing the calcination temperature. However, no obvious difference in particle size between C-500 and T-500 indicated that doping did not influence the crystal growth.

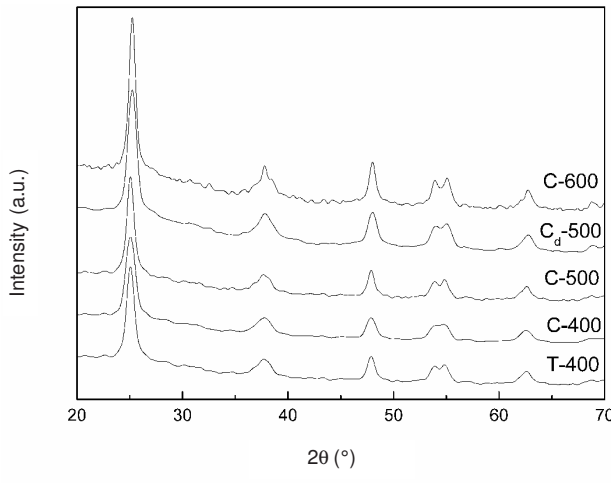

Fig. 1. XRD patterns of neat and carbon doped TiO_2 samples

Fig. 2 shows the TEM image (above) and high magnification image (below) of C-500. From the images, it is indicated that the particle sizes of C-500 were around 10 nm with the narrow particle size distribution. These are consistent with the XRD results. The ordered lattices were shown in high magnification image indicated that C-500 was composed of highly ordered crystalline particles.

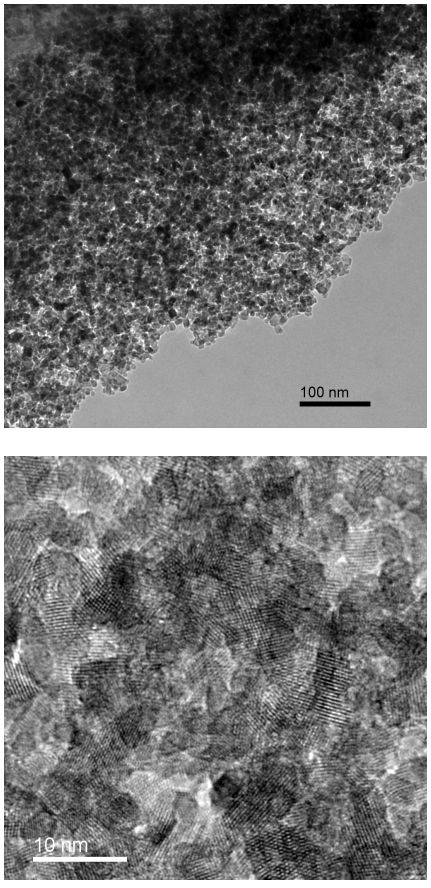

Fig. 2. TEM image (above) and high magnification image (below) of C-500

UV-visible spectra of prepared TiO_2 are presented in Fig. 3. Enhanced light absorption intensity in the visible region are shown clearly for the obtained carbon doped TiO_2 samples. The band gap energies of TiO_2 samples were calculated according to the method of Oregan and Gratzel[9]. The results indicated that the band gap of pure anatase TiO_2, T-500, was 3.1 eV. For carbon doped samples, this value decreased to 3.05, 2.82, 2.78 and 2.77 eV for C_d-500, C-400, C-500 and C-600, respectively. Obviously, the direct calcination sample, C_d-500, showed the much higher band gap than other samples which prepared by temperature-programmed calcination method. This result demonstrated that the calcination method strongly influence the doping of carbon.

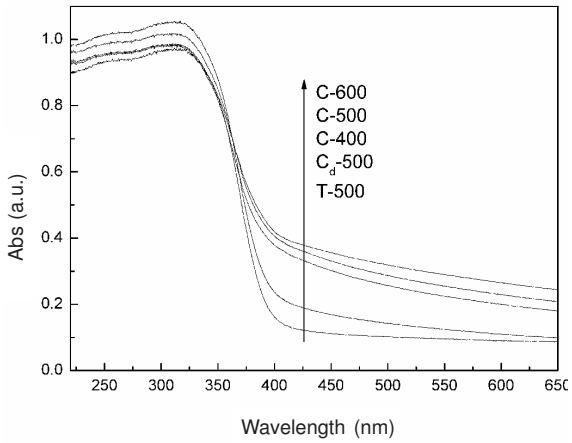

Fig. 3. UV-visible diffuse reflectance spectra of neat and carbon doped TiO_2 samples

Fig. 4 shows the XP spectra of T-500, C-500 and C_d-500 in the region of Ti 2p (A), O 1s (B) and C 1s (C). In the Ti 2p region (Fig. 4A), both T-500 and C-500 exhibited two peaks located at 458.5 and 464.2 eV respectovely, which could be assigned to Ti^{4+} $2p_{3/2}$ and Ti^{4+} $2p_{1/2}$. For O 1s region (Fig. 4B), the peaks around 530.3 and 532.5 eV for T-500 are attributed to crystal lattice oxygen (Ti-O) and surface hydroxyl group (O-H) of TiO_2[10]. For C-500, the peak assigned to crystal lattice oxygen showed an obvious shift to higher binding energy (530.6 eV). This is probably due to the electron donor capacity decreased after carbon doping, leading to the electron density of oxygen decreased, thus the binding energy of oxygen increased. Besides, the ratio of these two peak areas (S_{O-H}/S_{Ti-O}), which could be calculated from XPS data, represents the abundance of surface hydroxyl groups. The result showed that the S_{O-H}/S_{Ti-O} ratios for C-500 and T-500 were 0.23 and 0.12, respectively. This indicated more hydroxyl groups existed on C-500 surface.

For C 1s region, three peaks located at 284.6, 286.1 and 288.6 eV were observed. Those peaks located at 284.6 and 286.1 eV are attributed to the C-C group and the C-OH group of citric acid, respectively[11]. It has been addressed by several investigations where XPS analysis particularly has been used to reveal the two binding energy positions with C doped TiO_2 at 282 and 288.6 eV[12-14], which was attributed to Ti-C and Ti-O-C structure, respectively. Therefore, this small peak at higher binding energy (288.6 eV) was attributed to the electron-deficiency of the C atom in the Ti-O-C structure. However,

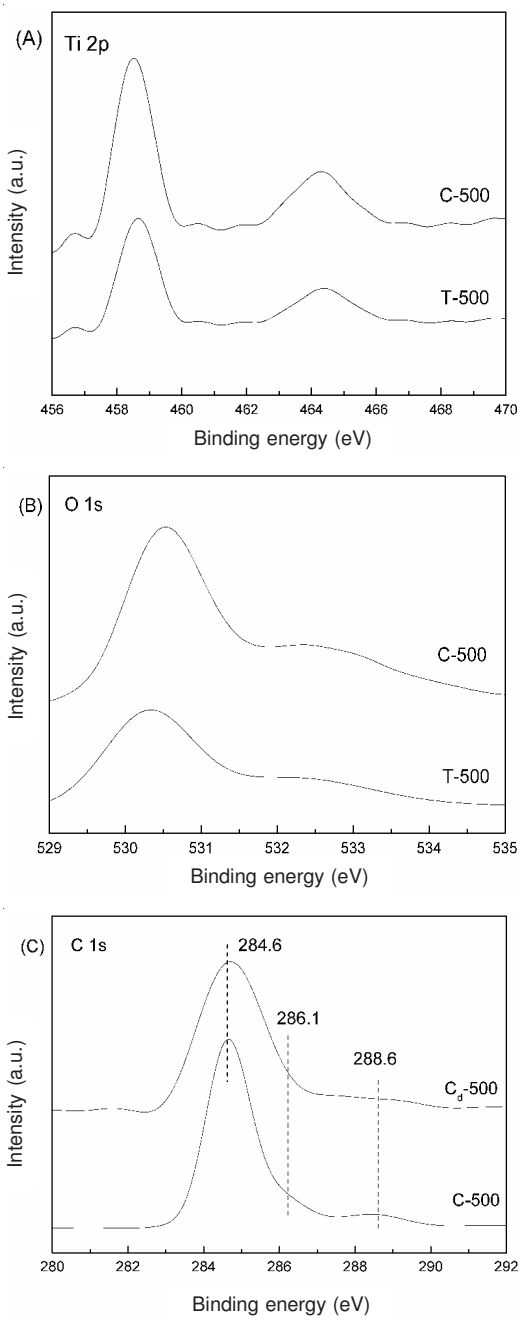

Fig. 4. XP spectra of T-500, C-500 and C_d-500 in the region of Ti 2p (A), O 1s (B) and C 1s (C)

compared with C-500, the peak intensity located at 288.6 eV decreased obviously for the sample C_d-500. This indicated that the doping content of carbon for C_d-500 was much lower than that of C-500. This result demonstrated that the calcination method strongly influence the doping of carbon, which is consistent with UV-visible result. Comparation of two preparation methods of C-500 and C_d-500, it is deduced that the doping of carbon occured mainly in the stage of 180 ºC maintenance. It is known that citric acid is decomposed at 175 ºC. For the preparation procedure of C-500, the sample was heated to 180 ºC and maintained for 2 h. Therefore, the citric acid could be decomposed slowly. However, for C_d-500, the sample was heated to 500 ºC directly, leading to the rapid decomposition of citric acid. Thus, the doping content of carbon of C-500 was much higher than that of C_d-500.

It is deduced that the gas produced from citric acid decomposition could overflow from the bulk of catalyst. Therefore, some mesoporous structure should be formed on the catalyst surface. The result of nitrogen adsorption indicated that the S_{BET} of T-500 was 62 $m^2 g^{-1}$. However, for the carbon doped samples, the S_{BET} were 198, 172, 164 and 131 $m^2 g^{-1}$ for C_d-500, C-400, C-500 and C-600, much higher than that of T-500. It is known that the small particle size of catalyst leads to the high S_{BET}. However, no obvious difference on particle size was observed between T-500 and carbon doped TiO_2. Therefore, it is deduced that some mesoporous structure should be formed on the surface of carbon doped TiO_2, leading to the high S_{BET}. Besides, the S_{BET} decreased rapidly when increased the calcination temperature, which might be attributed to the agglomeration among the particles and the pore collapse.

Fig. 5 shows the photocatalytic performances of neat and carbon doped TiO_2 samples in the degradation methylene blue under visible light irradiation. For neat TiO_2, T-500, the degradation percentage was only 12 % after 180 min. For C_d-500, prepared by heating to 500 ºC directly, the activity increased slightly. However, for the catalysts prepared by temperature-programmed calcination method, the degradation percentages were obviously increased. Among them, C-500 showed the highest activity. It is reported that the phase composition and particle size of TiO_2 have significant influence on its photocatalytic activity[15]. However, no obvious change were observed in phase compositions and particle sizes between T-500 and the samples prepared by temperature-programmed calcination method, indicating the enhanced photocatalytic activity must result from the doping of carbon in TiO_2, which gave rise to the narrowed band gap and thus to the enhanced absorption in the visible region. This indicated that the absorption of visible region is the primary factor for the photocatalytic activity under visible light. Besides, C-500 which exhibited the highest S_{BET} showed the highest degradation percentage. This indicated that S_{BET} also plays an important role in the photocatalytic activity under visible light.

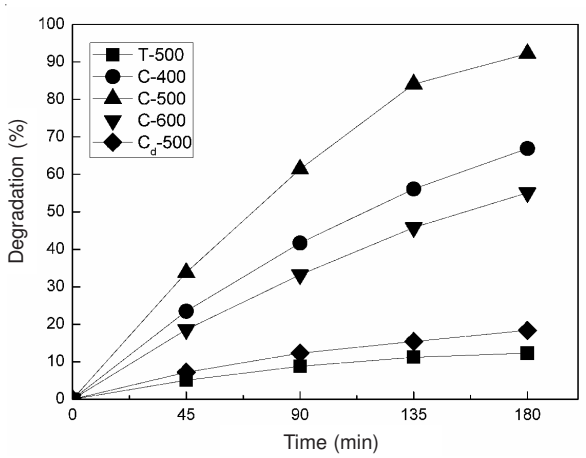

Fig. 5. Photocatalytic performances of neat and carbon doped TiO_2 samples in the degradation of methylene blue under visible light irradiation

Conclusion

Carbon doped mesoporous TiO_2 was prepared by temperature-programmed calcination method. Citric acid was used as not only carbon source but also the pore-forming agent. Carbon doping did not change the phase composition and particle sizes of TiO_2 samples, but extended its absorption edges to the visible light region. The XPS result indicated that the carbon doping content of sample prepared by temperature-programmed calcination method was much higher than that of C_d-500, which prepared by heating to 500 ºC directly. Under visible light, carbon doped mesoporous TiO_2 prepared by temperature-programmed calcination showed much higher photocatalytic activity than that of catalyst prepared by heating to 500 ºC directly and neat TiO_2. This is probably due to the doping of carbon into TiO_2 crystal lattice, which gave rise to the narrowed band gap and thus to the enhanced absorption in the visible region.

ACKNOWLEDGEMENTS

This work was supported by National Natural Science Foundation of China (No. 41071317, 30972418), National Key Technology R & D Programme of China (No. 2007BAC16B07, 2012ZX07505-001), the Natural Science Foundation of Liaoning Province (No. 20092080).

REFERENCES

1. R. Asahi, T. Morikawa, T. Ohwaki, A. Aoki and Y. Taga, *Science*, **293**, 269 (2001).
2. S.Z. Hu, F.Y. Li and Z.P. Fan, *J. Hazard. Mater*., **196**, 248 (2011).
3. T. Tachikawa, S. Tojo, K. Kawai, M. Endo, M. Fujitsuka and T. Ohno, *J. Phys. Chem. B*, **108**, 19299 (2004).
4. S. Klosek and D. Raftery, *J. Phys. Chem. B*, **105**, 2815 (2001).
5. M. Anpo and M. Takeuchi, *J. Catal*., **216**, 505 (2003).
6. S. Sakthivel and H. Kisch, *Angew. Chem. Int. Ed*., **42**, 4908 (2003).
7. H. Irie, Y. Watanabe and K. Hashimoto, *Chem. Lett*., **32**, 772 (2003).
8. J. Lin, Y. Lin, P. Liu, M.J. Meziani, L.F. Allard and Y.P. Sun, *J. Am. Chem. Soc*., **124**, 11514 (2002).
9. B. Oregan and M. Gratzel, *Nature*, **353**, 737 (1991).
10. S.Z. Hu, A.J. Wang, X. Li, Y. Wang and H. Löwe, *Chem. Asian J*., **5**, 1171 (2010).
11. S. Biniak, G. Szymanski, J. Siedlewski and A. Swiatkowski, *Carbon*, **35**, 1799 (1997).
12. I. Kang, Q.W. Zhang, S. Yin, T. Sato and F. Saito, *Appl. Catal. B*, **80**, 81 (2008).
13. W. Ren, Z. Ai, F. Jia, L. Zhang, X. Fan and Z. Zou, *Appl. Catal. B*, **69**, 138 (2007).
14. X.Y. Li, D.S. Wang, G.X. Cheng, Q.Z. Luo, J. An and Y.H. Wang, *Appl. Catal. B Environ*., **81**, 267 (2008).
15. M.R. Hoffmann, S.T. Martin, W. Choi and D.W. Bahnemann, *Chem. Rev*., **95**, 69 (1995).